THE ASTRONOMICAL JOURNAL VOLUME 107, NUMBER 3 MARCH 1994

TEST OF UNIFIED SCHEMES USING JET OPENING ANGLES

BEN R. OPPENHEIMER
Columbia Astrophysics Laboratory, Columbia University, New York, New York 10025
Electronic mail: boppenhe@odyssey.phys.columbia.edu

JOHN A. BIRETTA
Space Telescope Science Institute, 3700 San Martin Drive, Baltimore, Maryland 21218
Electronic mail: biretta@stsci.edu

Received 1993 June 21; revised 1993 November 10

ABSTRACT

Unified schemes attempt to classify radio loud quasars and Fanaroff–Riley Class II radio galaxies as a single type of object, whose properties depend on the orientation of the jet axis relative to the line of sight. We describe a new test of such unification schemes using observed jet opening angles as orientation indicators and apply it to existing data. Opening angles were measured for a subset of the 3CR catalogue, consisting of all identified extragalactic sources with $P_{178\ \mathrm{MHz}} > 10^{25}$ W/Hz and for which high resolution radio maps were found. This provided a sample relatively free of orientation effects. The observed distributions of opening angles for the quasars were compared with those of the galaxies, and with Monte Carlo simulations. We find that the observed jet opening angles of quasars tend to be larger than those of the galaxies; this result is consistent with, and supports, the unified scheme. Detailed Monte Carlo simulations suggest the observations are inconsistent with a simple unified scheme where a single orientation angle sharply distinguishes between quasars and galaxies. We modify Barthel's [ApJ, 336, 606 (1989)] unification scheme by introducing a range of orientation angles that differentiate quasars from galaxies; this yields more consistent results. However, neither Barthel's unification, nor the modification presented here, are fully able to account for the observed differences in quasar and galaxy redshift distributions. Finally, we demonstrate the existence of a loose anticorrelation between jet opening angle and source linear size, confirming that these parameters are useful as orientation indicators.

I. INTRODUCTION

Recently, attempts have been made to classify Fanaroff–Riley Class II radio galaxies (FRIIs) and radio loud quasars (QSRs) as the same type of object. This sort of unification is based on the premise that FRIIs and QSRs emit anisotropic radiation, with the great majority of the radiation directed along their jet's axis. Unification schemes propose that the differences between QSRs and FRIIs are merely artifacts of the orientation of their jets relative to the line of sight. In particular, Barthel (1989) suggests that all QSRs are oriented with their jets within 44.4° of the line of sight, and all FRIIs are oriented with their jets outside of this cone. It is this scheme which we test here.

Naturally, confirmation of the scheme would be exciting and provide insight into the astrophysics of QSRs and FRIIs. Alternatively, refutation of the scheme would indicate that the physical processes in QSRs and FRIIs are perhaps more disparate than similar and, thus, ill suited for explanation through orientation effects alone.

Several empirical tests of this scheme can be imagined rather quickly, and a few have been conducted. Of note are the test by Padovani & Urry (1992) using comparisons of luminosity functions and that of Barthel (1989) using linear size as an orientation indicator. Here we present another test using the observed opening angles of the jets as orientation indicators. The opening angles are likely to suffer somewhat different environmental effects than the source linear size, and might, therefore, eliminate the possibility that quasar-galaxy differences are related to environment rather than orientation.

2. THE TEST

Given a sample of FRIIs and QSRs that is unbiased by orientation with respect to the line of sight, one should see a distinct difference between the distributions of observed opening angles for quasars and for galaxies. The distributions should be different, if the unification scheme is correct in asserting that QSR jets are directed within 44.4° of the line of sight, because the observed opening angle of the jet is a function of its orientation with respect to that line of sight: Due solely to projection effects, a jet, modeled as a cone emanating from the core of the source, should appear wider when pointed towards the observer than when directed perpendicular to the line of sight (see Fig. 1). The observed opening angle is merely the projection of the intrinsic opening angle—that is, the angle of the cone used to model the jet—onto the plane of the sky. The two are related by the following equation derived from the geometry at issue:

$$\phi_{\mathrm{obs}} = 2 \arctan\left(\frac{\tan(\phi_i/2)}{\sin\theta}\right), \qquad (1)$$

 0004-6256/94/107(3)/892/12/$0.90

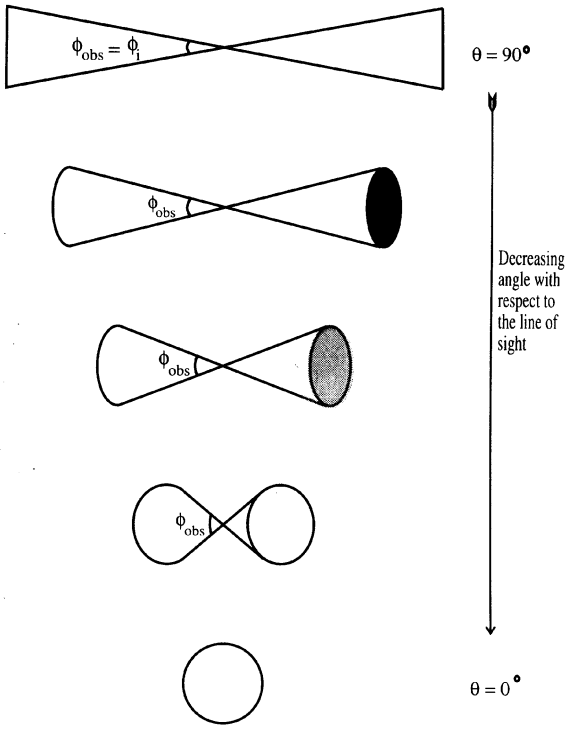

FIG. 1. Projection of conical jet onto plane of sky as function of orientation angle θ between jet axis and line of sight. The apparent opening angle increases as the jet is pointed more towards the observer.

where ϕ_{obs} is the observed opening angle, ϕ_i is the intrinsic opening angle, and θ is the angle between the jet and the line of sight.

Comparison of the two distributions of observed opening angles should reveal whether radio galaxy jets are all at large angles to the line of sight, as the model dictates: The distributions should reflect the fact that the radio galaxies have smaller observed opening angles than the quasars. Comparison of these distributions with distributions produced by a Monte Carlo simulation should yield measurements of how well the observations fit the unification scheme.

3. MEASUREMENT TECHNIQUE

Measurement of the jet opening angle involves measuring the FWHM of the jet at a number of distances along the jet, and deconvolving these measurements with the resolution of the map. A line is then fitted to a plot of the distances from the nucleus versus FWHM at those distances (both in arcsec). The slope of this best-fit line is the opening angle we used. This line fitting method provides a fairly straight forward "average" of the set of width measurements. This procedure is equivalent to fitting an idealized cone to the jet and measuring the opening angle of that cone.

A number of the sources studied had extremely faint jets which did not show themselves in the images available. From these sources we were able to measure only an upper limit on the opening angle of the jet. This was done by measuring the FWHM of the hot spot in the lobe. The hot spot in the lobe is a bright point at the terminating end of the jet. Based on examination of the radio maps in which both jets and their hot spots occur, it seems to be a valid assumption that the jet is not wider than the hot spot at the distance of the hot spot from the nucleus. So this single set of width and distance provided an upper limit on the opening angle. In cases where there were two hot spots of similar prominence, we used the average of the two opening angles so derived.

4. SOURCE SELECTION

It is of paramount importance for the success of this test that the sources used are not selected with any bias related to their orientations. In light of this, we decided to use a sample of sources which is flux limited at low frequencies. The decision to use low frequencies was made to avoid selecting sources by their beamed radiation which is emitted primarily by the jets and is, thus, anisotropic. The low frequency emissions are dominated by the lobes, the large diffuse radio structures at the terminating ends of the jets. This low frequency emission is assumed to be isotropic.

The second criterion used for selecting sources was a luminosity limit at this same low frequency. All sources in the final sample have luminosities greater than 10^{25} W/Hz at 178 MHz. This was introduced to eliminate FRI radio sources, since the unification scheme deals only with the FRII sources. A few FRI sources did get past this luminosity cut. This is due to the fact that the luminosity limit is not a strict demarcation between FRIs and FRIIs. Those FRIs that got through the cut were removed individually by visual inspection: Those sources with the FRI morphology were simply excluded from the sample.

These criteria were applied then to the revised 3CR catalogue, perhaps the most thorough flux-limited sample of radio sources. We threw out all galactic sources in this sample and the 36 optically unidentified sources, due to obscurations and other such problems. The final sample contained 237 sources, 52 of which are quasars. Approximately 25% of these have been mapped at high resolution and published. Hence, jet opening angles were measured for 45 galaxies and 17 quasars.

About five or six QSRs and FRIIs were excluded from the study because their morphologies were simply too complicated to lend themselves to opening angle measurements. Data for all sources in our sample are listed in Table 1, and resultant distributions are shown in Fig. 2. As one can read in Table 1, more than half the galaxy data are upper limits (indicated on the distributions in Fig. 2 by "<" symbols). These upper limit points could conceivably pose difficulties when interpreting the data. Nonetheless, we include them since some of the limits are fairly low, and, therefore, contain useful information. We present, as a simple, "first glance" at the data, the median opening angles for the galaxies and the quasars, calculated both with and without the upper limit values:

TABLE 1. Radio sources and measured jet opening angles.

3C	z	S_{178}	t	ϕ	P_{178}	LAS	Lin.	Ref.	Notes	3C	z	S_{178}	t	ϕ	P_{178}	LAS	Lin.	Ref.	Notes
2.0	1.0370	14.9	q	6.3	28.6	9.8	56	1	4	274.1	0.4220	16.5	g	<16.4	27.8	150.2	661	7	1
9.0	2.0120	17.8	q	3.2	29.3	15.2	83	28	4	277.3	0.0857	9.0	g	5.6	26.1	40.4	58	11	1,2
16.0	0.4050	11.2	g	<16.3	27.6	47.4	204	31	1	280.1	1.6590	9.2	q	2.8	28.9	15.3	86	28	3
22.0	0.9370	12.1	g	2.5	28.4	27.3	153	2	4	286.0	0.8490	25.0	q	6.6	28.7	4.6	26	9	3
33.1	0.1810	13.0	g	<13.8	26.9	176.5	462	23	1	287.1	0.2159	8.2	n	< 3.3	26.9	125.0	371	32	1,2
35.0	0.0670	10.5	g	<16.6	26.0	573.4	665	23	1	293.0	0.0452	12.7	g	3.2	25.7	166.8	135	16	2
40.0	0.0177	26.0	g	< 3.0	25.2	289.2	96	32	1	299.0	0.3670	11.8	g	14.2	27.5	0.9	4	26	2
43.0	1.4700	11.6	q	6.7	28.9	0.4	2	26	5	305.0	0.0410	15.7	g	5.3	25.7	2.4	2	14	2
47.0	0.4250	26.4	q	6.1	28.0	87.1	384	3	5	309.1	0.9040	22.7	q	<24.8	28.7	2.6	15	31	1
49.0	0.6210	10.3	g	< 6.3	28.0	1.3	6	29	1,2	318.0	0.7520	12.3	n	< 7.4	28.2	1.1	6	26	1,2
52.0	0.2854	13.5	g	7.5	27.4	96.7	344	4	1,2	323.1	0.2640	9.7	q	< 2.0	27.2	80.7	274	27	1
55.0	0.7350	21.5	g	1.3	28.3	68.3	367	2	1,3	324.0	1.2063	15.8	g	< 3.9	28.8	10.0	57	2	4
66.0	0.0215	24.6	g	<12.1	25.3	16.9	6	25	1,2	327.0	0.1039	35.3	g	< 3.4	26.9	673.9	1141	32	1
79.0	0.2559	30.5	n	< 1.6	27.6	97.3	323	32	1	332.0	0.1515	9.6	g	< 7.2	26.7	265.6	609	32	1
99.0	0.4260	10.8	n	7.4	27.6	6.7	29	6	3	338.0	0.0298	46.9	g	<19.2	25.9	45.3	25	18	1
103.0	0.3300	26.6	g	< 3.8	27.8	92.4	358	4	2	345.0	0.5940	10.8	q	8.5	28.0	7.1	36	12	4
109.0	0.3056	21.6	n	< 1.4	27.6	95.5	354	32	1	346.0	0.1610	10.9	g	< 4.5	26.8	4.1	10	26	1
111.0	0.0485	64.6	g	2.0	26.5	140.8	121	24	8	352.0	0.8057	11.3	g	4.1	28.3	12.1	66	2	4
138.0	0.7590	22.2	q	3.7	28.5	0.8	5	29	1,3	356.0	1.0790	11.3	g	< 1.6	28.5	96.3	550	2	1
165.0	0.2900	13.5	g	8.5	27.4	66.8	240	4	1	357.0	0.1664	9.7	g	< 8.4	26.7	95.4	235	17	1
171.0	0.2384	19.5	n	< 4.6	27.4	17.5	55	32	1	371.0	0.0500	3.7	n	11.3	25.3	46.5	41	19	4
186.0	1.0630	14.1	q	2.6	28.6	4.4	25	26	3	381.0	0.1605	16.6	g	< 1.3	26.9	60.8	146	32	1
190.0	1.1970	15.0	q	1.9	28.7	5.2	30	26	1,2	390.3	0.0561	47.5	n	< 7.8	26.5	219.0	217	23	1
194.0	0.3120	9.9	g	< 7.9	27.3	12.5	47	7	1	405.0	0.0565	8700.0	g	1.7	28.7	59.9	60	13	6
219.0	0.1744	41.2	g	2.9	27.5	34.9	89	30	8	418.0	1.6860	13.1	q	7.2	29.0	4.2	24	22	3
223.0	0.1368	14.7	g	<11.1	26.7	197.4	418	23	1	424.0	0.1270	14.6	g	< 1.6	26.7	17.1	34	33	1,6
236.0	0.0989	14.4	g	< 0.7	26.5	64.0	208	8	3	433.0	0.1016	56.2	g	2.6	27.1	47.0	78	33	4
245.0	1.0290	14.4	q	< 2.4	28.6	5.7	33	9	2,1	452.0	0.0811	54.4	g	< 1.5	26.9	257.8	354	33	1
265.0	0.8110	19.5	g	< 2.0	28.5	149.0	820	2	1	454.0	1.7570	11.6	q	7.0	29.0	0.5	3	26	4
268.2	0.3620	9.7	g	<19.5	27.5	27.6	112	7	1	454.3	0.8600	13.0	q	9.8	28.4	10.4	58	21	3
273.0	0.1580	62.8	q	3.2	27.5	41.7	99	10	6	465.0	0.0293	37.8	g	4.1	25.8	80.4	43	20	5

Notes to TABLE 1

3C indicates the number of the source in the 3C catalog. z is the source's redshift. t indicates whether the source is a galaxy (g), and n-type galaxy (n) or a quasar (q). S_{178} is the flux density of 178 MHz radiation from the source in Jy. ϕ indicates the opening angle we measured for this source. P_{178} is the log of the 178 MHz luminosity of the source in W/Hz. The Hubble constant is assumed to be 75 km/s/Mpc, and q_0 to be 0.5 for the calculation of these luminosities. LAS is the largest angular size of the object in arcseconds. Lin. is the corresponding linear size in kpc.

1. This measurement was made only with a hot spot or two.
2. This measurement is the average of two points along the jet.
3. This measurement is the average of three points.
4. This measurement is the average of four points.
5. This measurement is the average of five points.
6. This measurement is the average of six points.
8. This measurement is the average of eight points.

References to TABLE 1

1. Saikia *et al.* (1987).
2. Fernini (1992).
3. Fernini *et al.* (1991).
4. Pooley *et al.* (1987).
5. Owen *et al.* (1985).
6. Mantovani *et al.* (1990).
7. Strom *et al.* (1990).
8. Barthel *et al.* (1985).
9. Saikia *et al.* (1990).
10. Davis *et al.* (1985).
11. Bridle *et al.* (1981a).
12. Kollgaard *et al.* (1989, 1990).
13. Perley *et al.* (1984).
14. Heckman *et al.* (1982).
15. van Breugel & Fomalont (1984).
16. Bridle *et al.* (1981b).
17. Fanti *et al.* (1987).
18. Burns *et al.* (1983).
19. Wrobel & Lind (1990).
20. Eilek *et al.* (1984), Leahy (1984).
21. Browne *et al.* (1982).
22. O'Dea *et al.* (1988).
23. Jaegers (1987).
24. Linfield & Perley (1984).
25. Leahy *et al.* (1986).
26. Spencer *et al.* (1991).
27. Swarup *et al.* (1984).
28. Swarup *et al.* (1982).
29. Fanti *et al.* (1989).
30. Bridle *et al.* (1986).
31. Pearson *et al.* (1985).
32. Antonucci (1985).
33. Black *et al.* (1992).

$(\overline{\phi_{\rm obs}})_{\rm galaxies}=4.6°$ and $(\overline{\phi_{\rm obs}})_{\rm quasars}=6.3°$

(upper limit data included),

$(\overline{\phi_{\rm obs}})_{\rm galaxies}=4.1°$ and $(\overline{\phi_{\rm obs}})_{\rm quasars}=6.1°$

(upper limit data excluded).

This first glance at the data shows that the quasars, in general, have larger opening angles than the galaxies, which is what is predicted by the unification scheme. Clearly, there are no radical changes when the upper limit data are excluded. One should, however, bear in mind that the redshift distributions of the galaxies and quasars are quite different (Fig. 3). The statistical significance of these results, and the effects of cosmic evolution, are discussed below.

5. THE MONTE CARLO MODEL AND ITS COMPARISON WITH OBSERVED OPENING ANGLES

In order to provide quantitative comparison of the observed data with the Barthel unification scheme, a Monte Carlo model of the scheme was produced. This model randomly generates 100 000 intrinsic opening angles (within a small range) and randomly assigns to each an orientation angle. The orientation angles have a quarter-sine-wave distribution, so that there are more orientated perpendicular to the line of sight and very few parallel to the line of sight, as is required by the geometry of the situation.

After these 100 000 pairs of angles—each consisting of an intrinsic opening angle and its assigned orientation angle—are generated, each pair is designated to be a "galaxy" or a "quasar," depending solely on the orientation angle. If the orientation angle is less than 44.4°, the pair is called a quasar, and at larger angle it is designated a galaxy, per Barthel's unification scheme. (Herein we will call this angle which distinguishes between galaxies and quasars the cutoff angle, or θ_c.) Once each pair of angles has been designated a galaxy or quasar, an "observed" or "apparent" opening angle is calculated using Eq. (1) above. The distribution of these 100 000 apparent opening angles is plotted in Fig. 4, where separate panels are used for those designated to be galaxies and those designated to be quasars.

Comparison of the observed distributions against the simulated ones is not an easy task. A simple Kolmogorov–Smirnoff test, often useful for comparing two distributions, is not truly insightful here, since there are, in fact, two sets of two distributions to be compared (the observed galaxy and quasar distributions versus the model's galaxy and

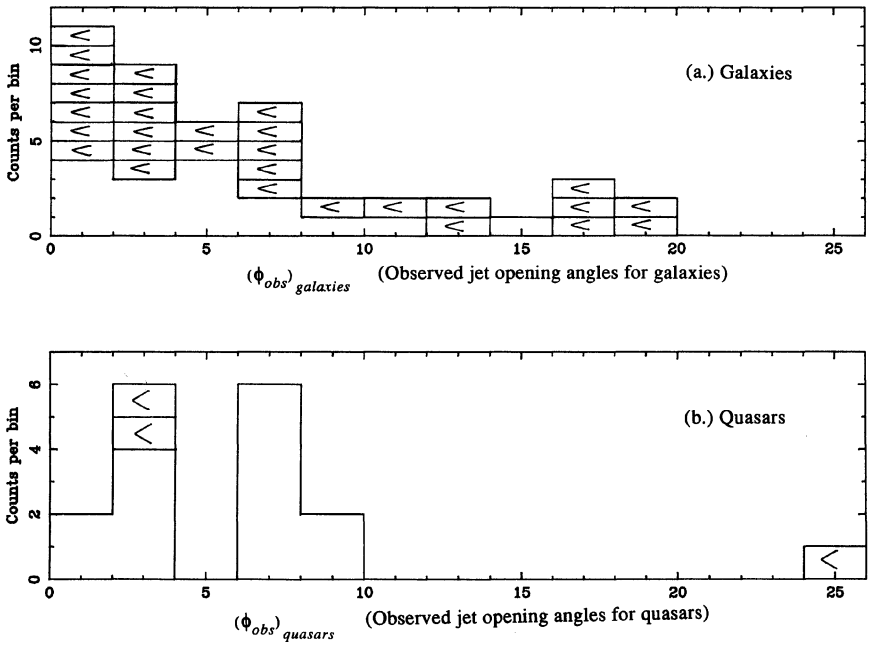

FIG. 2. Distributions of observed jet opening angles ϕ_{obs} for (a) galaxies and (b) quasars. Opening angles which are upper limits are marked with < symbols.

quasar distributions). Instead, we calculated the median opening angle for the quasar distribution, $\overline{\phi_q}$, the median opening angle for the galaxy distribution, $\overline{\phi_g}$, and finally the ratio of these medians,

$$R \equiv \frac{\overline{\phi_q}}{\overline{\phi_g}}. \quad (2)$$

It is these ratios which we will use to compare the observed and simulated distributions. We used medians instead of means, to prevent the large upper limit values from having too much influence on the calculated ratios.

Part of the problem of comparing the observations and models involves the question of how to incorporate best the measured opening angles which are merely upper limits.

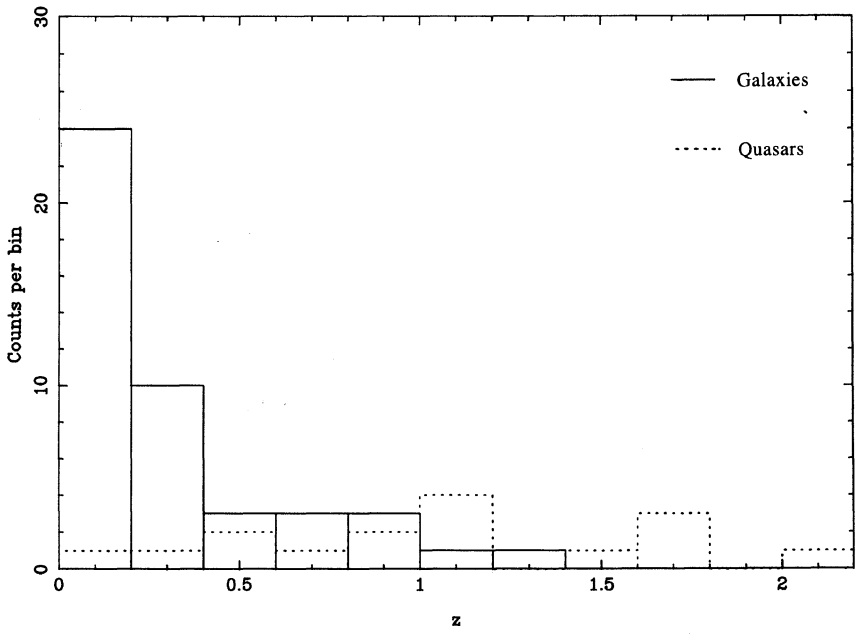

FIG. 3. Redshift distribution of galaxies (solid line) and quasars (dotted line) in the observed sample.

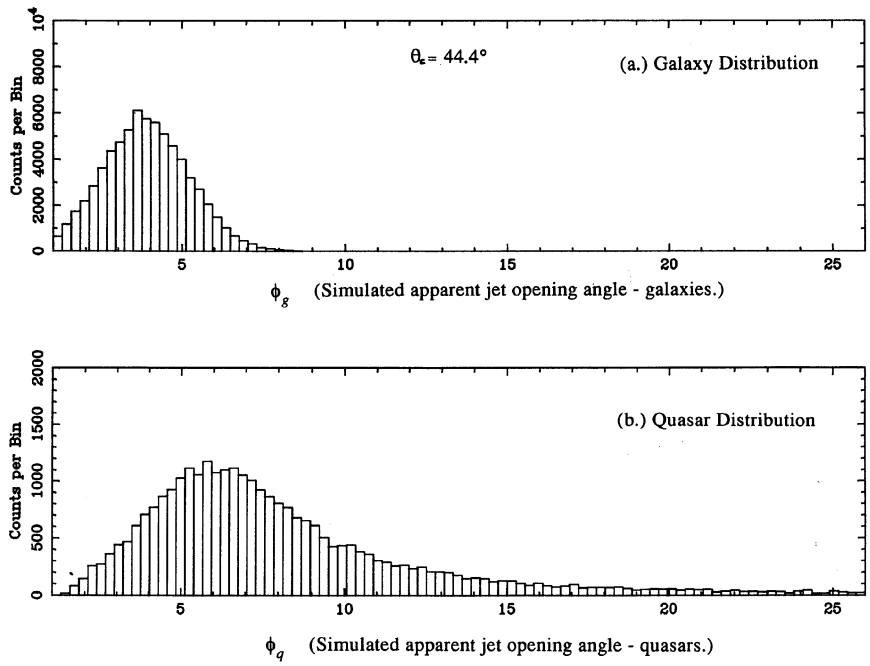

FIG. 4. Distributions of observed (apparent) jet opening angles for Monte Carlo simulation with sharp cutoff angle at $\theta_c = 44.4°$. A total of 100 000 jets are contained in the simulation. (a) Distribution for galaxies. (b) Distribution for quasars.

More than half of the galaxy data are upper limits (indicated on the Fig. 2 distributions by < symbols). As we mentioned, some of these upper limits are fairly low, and contain useful information. We simply present the ratios of median opening angles calculated both with, and without, the upper limit values. The observed ratios are thus

$$R_{\rm obs} = \frac{6.3°}{4.6°} = 1.37 \quad \text{(upper limit data included)},$$

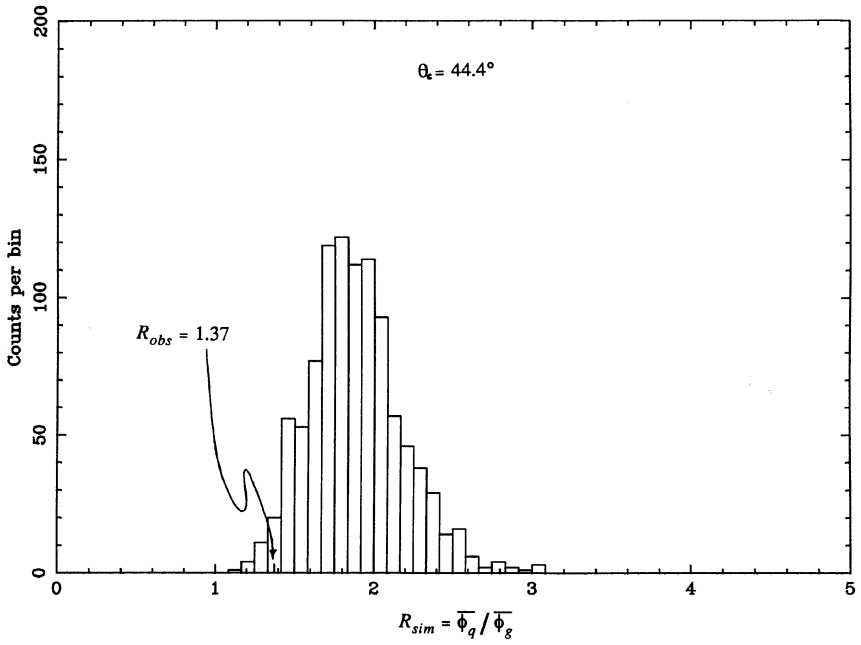

FIG. 5. Distribution of Monte Carlo simulated ratios $R_{\rm sim}$ assuming a sharp cutoff angle of 44.4°. One thousand ratios are shown, each computed for a sample of 45 galaxies and 17 quasars. The observed ratio $R_{\rm obs} = 1.37$ is indicated for objects in the redshift range $z = 0$–5, with opening angle upper limit values included (i.e., 45 galaxies and 17 quasars in sample).

TABLE 2. Summary of principle results.

(a) Monte Carlo simulation with sharp 44.4° cutoff angle.

z	G	Q	$\bar{\phi}_g$	$\bar{\phi}_q$	$\bar{z}_g$	$\bar{z}_q$	R_{obs}	$\bar{R}_{sim}$	σ	dev.	%<
[.0, 5.0]	45	17	4.6	6.3	.30	1.05	1.37	1.88	.29	1.75	92
[.0, 5.0][1]	16	14	4.1	6.1	.28	1.11	1.49	1.95	.32	1.44	83
[.3, 1.0]	14	5	7.4	6.6	.54	.70	.89	1.92	.62	1.66	90
[.3, 1.5]	16	10	6.3	6.3	.62	.93	1.00	1.99	.52	1.90	94
[.3, 2.0]	16	13	6.3	6.3	.62	1.11	1.00	1.85	.37	2.28	98
[.4, 1.0]	9	5	6.3	6.6	.66	.70	1.05	1.99	.73	1.29	81
[.4, 1.5]	11	10	4.1	6.3	.75	.93	1.54	2.06	.52	.99	68
[.4, 2.0]	11	13	4.1	6.3	.75	1.11	1.54	1.88	.39	.87	62
[.5, 1.0][2]	6	4	4.1	6.6	.78	.79	1.61	2.34	1.29	.57	43
[.5, 1.5]	8	9	3.9	6.3	.87	.98	1.62	1.97	.52	.67	49
[.5, 2.0]	8	13	3.9	6.6	.87	1.16	1.69	1.92	.50	.47	35

(b) Monte Carlo simulation with 44.4°±5° range of cutoff angles.

z	G	Q	$\bar{\phi}_g$	$\bar{\phi}_q$	$\bar{z}_g$	$\bar{z}_q$	R_{obs}	$\bar{R}_{sim}$	σ	dev.	%<
[.0, 5.0]	45	17	4.6	6.3	.30	1.05	1.37	1.86	.31	1.60	89
[.0, 5.0][1]	16	14	4.1	6.1	.28	1.11	1.49	1.90	.38	1.07	71
[.3, 1.0]	14	5	7.4	6.6	.54	.70	.89	1.89	.65	1.55	88
[.3, 1.5]	16	10	6.3	6.3	.62	.93	1.00	1.96	.49	1.98	95
[.3, 2.0]	16	13	6.3	6.3	.62	1.11	1.00	1.84	.36	2.33	98
[.4, 1.0]	9	5	6.3	6.6	.66	.70	1.05	1.94	.65	1.37	83
[.4, 1.5]	11	10	4.1	6.3	.75	.93	1.54	2.01	.51	.92	64
[.4, 2.0]	11	13	4.1	6.3	.75	1.11	1.54	1.89	.41	.85	60
[.5, 1.0][2]	6	4	4.1	6.6	.78	.79	1.61	2.25	.98	.65	48
[.5, 1.5]	8	9	3.9	6.3	.87	.98	1.62	1.96	.52	.64	48
[.5, 2.0]	8	13	3.9	6.6	.87	1.16	1.69	1.88	.44	.44	34

(c) Monte Carlo simulation with 44.4°±10° range of cutoff angles.

z	G	Q	$\bar{\phi}_g$	$\bar{\phi}_q$	$\bar{z}_g$	$\bar{z}_q$	R_{obs}	$\bar{R}_{sim}$	σ	dev.	%<
[.0, 5.0]	45	17	4.6	6.3	.30	1.05	1.37	1.77	.31	1.30	81
[.0, 5.0][1]	16	14	4.1	6.1	.28	1.11	1.49	1.84	.40	.86	61
[.3, 1.0]	14	5	7.4	6.6	.54	.70	.89	1.81	.66	1.40	84
[.3, 1.5]	16	10	6.3	6.3	.62	.93	1.00	1.88	.47	1.88	94
[.3, 2.0]	16	13	6.3	6.3	.62	1.11	1.00	1.76	.37	2.06	96
[.4, 1.0]	9	5	6.3	6.6	.66	.70	1.05	1.89	.70	1.21	77
[.4, 1.5]	11	10	4.1	6.3	.75	.93	1.54	1.94	.54	.75	55
[.4, 2.0]	11	13	4.1	6.3	.75	1.11	1.54	1.80	.44	.59	45
[.5, 1.0][2]	6	4	4.1	6.6	.78	.79	1.61	2.19	1.06	.55	42
[.5, 1.5]	8	9	3.9	6.3	.87	.98	1.62	1.87	.50	.50	38
[.5, 2.0]	8	13	3.9	6.6	.87	1.16	1.69	1.85	.47	.34	27

(d) Monte Carlo simulation with 44.4°±20° range of cutoff angles.

z	G	Q	$\bar{\phi}_g$	$\bar{\phi}_q$	$\bar{z}_g$	$\bar{z}_q$	R_{obs}	$\bar{R}_{sim}$	σ	dev.	%<
[.0, 5.0]	45	17	4.6	6.3	.30	1.05	1.37	1.48	.27	.41	32
[.0, 5.0][1]	16	14	4.1	6.1	.28	1.11	1.49	1.54	.34	.15	12
[.3, 1.0]	14	5	7.4	6.6	.54	.70	.89	1.55	.56	1.17	76
[.3, 1.5]	16	10	6.3	6.3	.62	.93	1.00	1.59	.44	1.36	83
[.3, 2.0]	16	13	6.3	6.3	.62	1.11	1.00	1.49	.34	1.42	84
[.4, 1.0]	9	5	6.3	6.6	.66	.70	1.05	1.56	.60	.85	60
[.4, 1.5]	11	10	4.1	6.3	.75	.93	1.54	1.63	.49	.19	16
[.4, 2.0]	11	13	4.1	6.3	.75	1.11	1.54	1.53	.36	.03	2
[.5, 1.0][2]	6	4	4.1	6.6	.78	.79	1.61	1.89	.97	.29	24
[.5, 1.5]	8	9	3.9	6.3	.87	.98	1.62	1.58	.46	.09	8
[.5, 2.0]	8	13	3.9	6.6	.87	1.16	1.69	1.53	.40	.40	31

Notes to TABLE 2

z is the redshift range used in calculating R_{obs}. G and Q are the number of galaxies in the sample and the number of quasars in the sample, respectively. These numbers are also used in the Monte Carlo model to generate the distribution of ratios. ϕ_g and ϕ_q are the median observed galaxy opening angle and the median observed quasar opening angle, respectively. $\bar{z}_g$ and $\bar{z}_q$ are the average redshift of the galaxies and of the quasars, respectively. R_{obs} is the ratio of the observed quasar opening angle to the observed galaxy opening angle. $\bar{R}_{sim}$ is the average ratio calculated by the Monte Carlo model. σ is the standard deviation of the distribution of ratios computed by the Monte Carlo model. dev. is the deviation of R_{obs} from $\bar{R}_{sim}$ in units of standard deviations. %< is the percentage of the ratio distribution computed by the Monte Carlo model which lies closer to $\bar{R}_{sim}$ than R_{obs} does.

[1]Upper limit values are not used in the values on this line, although they are used in all other data.

[2]Though the ratio is rather high in this case, the median quasar opening angle is chosen from a set of four values: 3.7, 6.6, 8.5, 9.8 (and a fifth, <24.8, if 3C309.1 is included). In this case, the median is not well defined, so the observed ratio could just as easily be 2.07.

$$R_{obs}=\frac{6.1°}{4.1°}=1.49 \quad \text{(upper limit data excluded)}.$$

The difference between these two values is small, indicating that inclusion of the upper limits should have little impact on the conclusions.

A further problem involves the uncertainties caused by the small number of observed objects. While the Monte-Carlo model (described above and plotted in Fig. 4) is based on 100 000 jets, the observed sample contains only 62. To provide a consistent comparison, and to estimate the probability that the observed jets and Monte Carlo "jets" are drawn from the same distribution, we computed the ratio R_{sim} [defined in Eq. (2)] for small samples of jets drawn randomly from the 100 000 in the Monte Carlo simulation. We then repeated this calculation 1000 times, so as to obtain a distribution of R_{sim}. For example, for a redshift range including all the observed data (z=0–5) and including the upper limit points, there are 45 galaxies and 17 quasars. To generate R_{sim} for this case we randomly selected 45 galaxies and 17 quasars from the Monte-Carlo simulation, and then repeated this 1000 times obtaining the R_{sim} distribution plotted in Fig. 5. Parameters for this example are also listed in the first row of Table 2(a).

Given the observed opening angle ratio R_{obs} and the distribution of Monte-Carlo ratios R_{sim} (Fig. 5) we can then attempt to quantify the probability that the observed opening angles and simulated ones are drawn from the same distributions. For this example including all the observed data (45 galaxies and 17 quasars in the sample), the observed ratio $R_{obs}=1.37$ falls near the bottom end of the R_{sim} distribution, indicating that agreement of the model and observations is somewhat improbable. One way to quantify this further is to parametrize the R_{sim} distribution by noting it has a mean $\bar{R}_{sim}=1.88$ and standard deviation $\sigma=0.29$ which places R_{obs} about 1.75 standard deviations from the mean ratio for the simulations. Another quantification is to note that 92% of the models in the distribution were closer to the mean $\bar{R}_{sim}=1.88$ than the observed value $R_{obs}=1.37$ [see Table 2(a)].

Restricting the redshift range of the observed jets reduces the quantities of galaxies and quasars, and hence requires simulations for smaller sample sizes. Simulations were run for a number of redshift restrictions using appropriate sample sizes. These results are summarized in Table 2(a). We also give results for a sample excluding the measured opening angles which are merely upper limits.

There are a number of degrees of freedom in Barthel's unification scheme. For instance, suppose we say all the quasars lie oriented within 75° of the line of sight, instead of 44.4°? This tends to make the observed galaxy and quasar opening angles more similar, so that the Monte Carlo ratios move towards unity, hence placing the observed ratios in the middle of the Monte Carlo ratio distribution. But this also produces far more quasars than galaxies, which is contrary to observation. Making the cutoff angle smaller than 44° only pushes the Monte Carlo ratioshigher, and therefore lessens the possibility that the unification scheme is consistent with the observations.

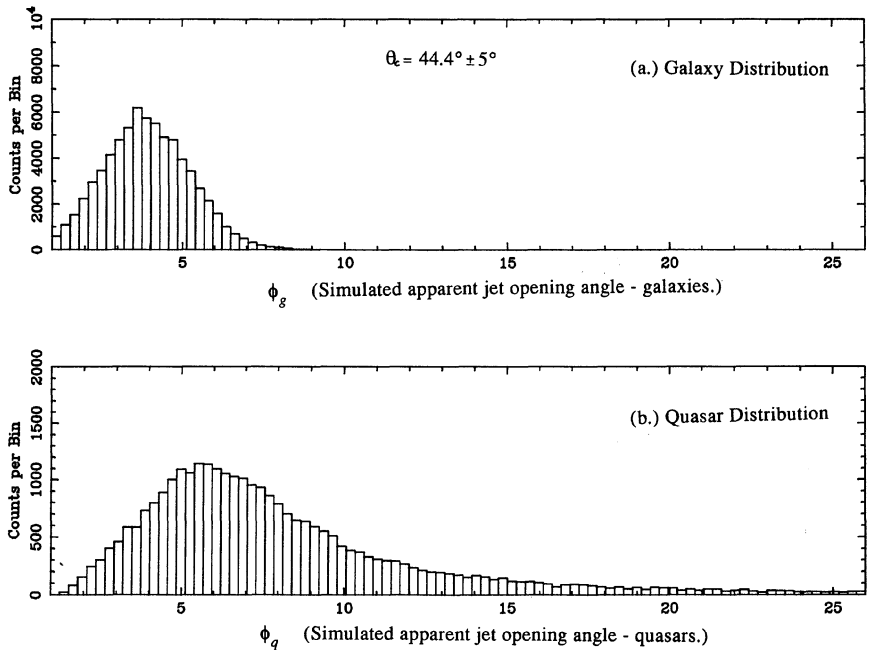

FIG. 6. Distributions of jet opening angles for Monte Carlo simulation with range of cutoff angles between $\theta = 39.4°$ and 49.4° ($\theta_c = 44.4° \pm 5°$). Other details are the same as Fig. 4.

Another degree of freedom is the set of intrinsic opening angles used in the Monte Carlo model. We have used a distribution of intrinsic angles which is uniform between 1° and 6°, since this caused the resulting model distributions to resemble, at least in magnitude and width, the observed distributions. Making this range smaller produced very narrow Monte Carlo angle distributions. Making it very broad spread out the Monte Carlo angle distributions. In neither case were the calculated ratios significantly altered.

Finally, we considered a modification of the unification scheme: Perhaps instead of a single, sharp cutoff angle, there is a range of cutoff angles such that an object oriented within this range could be classified as either a galaxy or quasar. For an object oriented within this range, there might be several ways of ascertaining, within the Monte Carlo model, what type of object it is. First, one could decide randomly, giving an object a 50% chance of being labeled a quasar. Second, one could decide randomly with a certain probability as a function of angle. That is, one might say that if the object's orientation is at the low end of the range, it should have a higher probability of being typed a quasar. We tried two such probability functions—a linear function and a half-sinusoidal function. These three methods of determining the type of object result in virtually the same conclusions with respect to the success of the unification model. Herein we show results for the first case, that is, where an object in the cutoff angle range has a 50–50 chance of being designated a quasar or a galaxy. The resulting distributions for a range cutoff angles between 39.4° and 49.4° ($\theta_c = 44.4° \pm 5°$) are shown in Figs. 6 and 7, and the results are summarized in Table 2(b). This range is not too large, and is in accordance with Barthel's (1989) specification that the cutoff angle is between 40° and 50°. Results for wider ranges of cutoff angle $\theta_c = 44.4° \pm 10°$ and $\theta_c = 44.4° \pm 20°$ are shown in Figs. 8–11, with summaries in in Tables 2(c) and 2(d). We finally note that if the range in cutoff angle is made too large, the unification model becomes a virtual triviality with objects being randomly designated as galaxies and quasars, and thus providing little insight into the astrophysics.

6. RESULTS AND DISCUSSION

Barthel's (1989) unified scheme predicts that double-lobed quasars and FRII galaxies are intrinsically identical objects, and differ only in their orientation relative to the observer's line of sight. In this scheme, objects appear to be quasars if the jet axis happens to be oriented near the line of sight, and otherwise they appear to be galaxies. If this model is correct, it further implies that quasars should appear to have broader jet opening angles than FRII galaxies. We have measured opening angles for a sample of 62 jets, and find this is indeed true. If we include all jets regardless of redshift, we find an observed ratio of median quasar opening angle to median galaxy opening angle, $R_{\rm obs} = 1.37$. Barthel used a redshift range $0.5 < z < 1.0$ in his work, and for this range we obtain a similar result, $R_{\rm obs} = 1.61$. This appears to give a rough confirmation of the unified scheme.

We have used Monte Carlo simulations to produce a more detailed comparison of the model and observation, and to test the statistical significance of the comparisons. Figure 4 shows the distributions of opening angles predicted for the simplest model with a sharp cutoff angle at 44.4°. These distributions are then used to simulate results for our sample size. Figure 5 shows the distribution of the

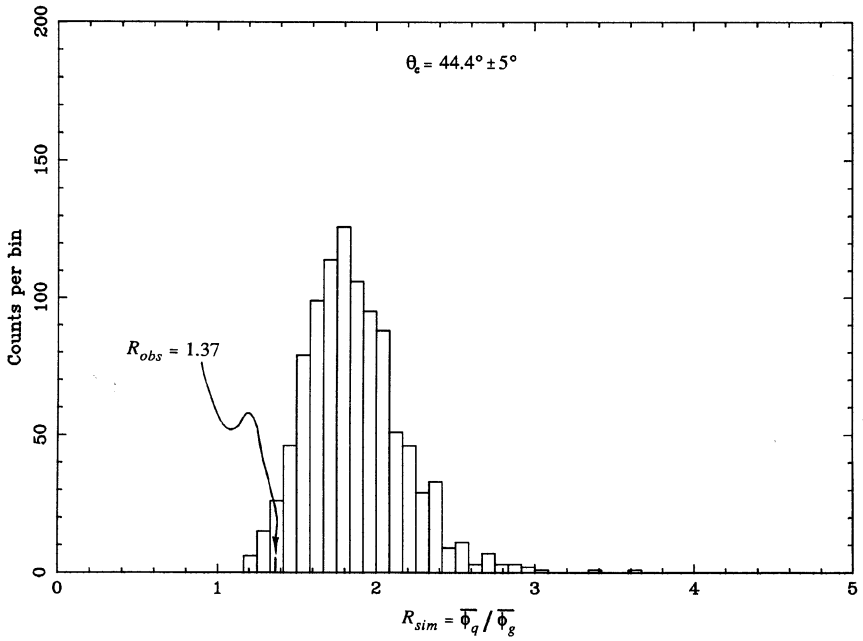

FIG. 7. Distribution of Monte Carlo simulated ratios R_{sim} assuming range of cutoff angles between $\theta=39.4°$ and 49.4° ($\theta_c=44.4\pm5°$). Other details are the same as Fig. 5.

ratios of median quasar opening angle to median galaxy opening angle for our sample consisting of 45 galaxies and 17 quasars. The observed ratio $R_{obs}=1.37$ falls near the bottom end of the predicted distribution, indicating the model predicts opening angles for the quasars which are too large in comparison to the galaxy opening angles. This discrepancy may be quantified by noting the observed ratio $R_{obs}=1.37$ falls 1.75 standard deviations ($\sigma=0.29$) below the average simulated ratio $\overline{R_{sim}}=1.88$, or put another way, 92% of the simulated ratios lie closer to the most probable ratio [Table 2(a)]. Hence, it seems somewhat unlikely that observations and simulations are drawn from the same model distribution. A variation is to exclude the observed angles which are merely upper limits, we obtain

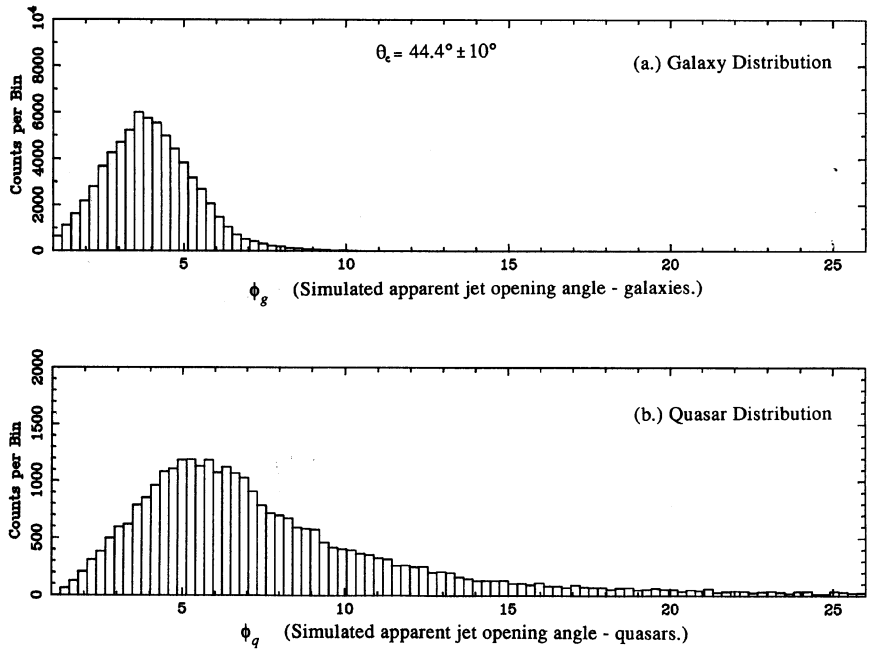

FIG. 8. Distributions of jet opening angles for Monte Carlo simulation with range of cutoff angles between $\theta=34.4°$ and 54.4° ($\theta_c=44.4°\pm10°$). Other details are the same as Fig. 4.

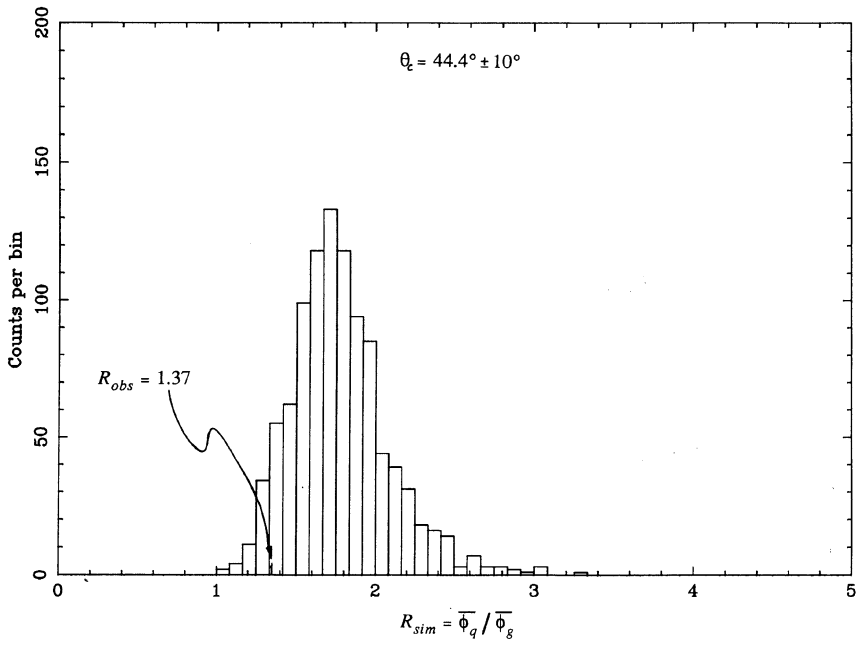

FIG. 9. Distribution of Monte Carlo simulated ratios $R_{\rm sim}$ assuming range of cutoff angles between $\theta=34.4°$ and 54.4° ($\theta_c=44.4\pm10°$). Other details are the same as Fig. 5.

the results in the second line of Table 2(a). This gives similar results with $R_{\rm obs}=1.49$, which lies about 1.44 standard deviations below the mean simulated ratio, placing 83% of the distribution closer to the mean. These results how that a naive version of the unified scheme having a sharp cutoff angle is probably inconsistent with observation.

If, instead of a sharp cutoff angle, we introduce a range of cutoff angles, the probability that the observations and simulations are drawn from the same distribution increases. Figures 6 and 7, along with Table 2(b), show results for a unified scheme wherein objects with an orientation angle between 39.4° and 49.4° may be classified as either quasars or galaxies. For the case where all observa-

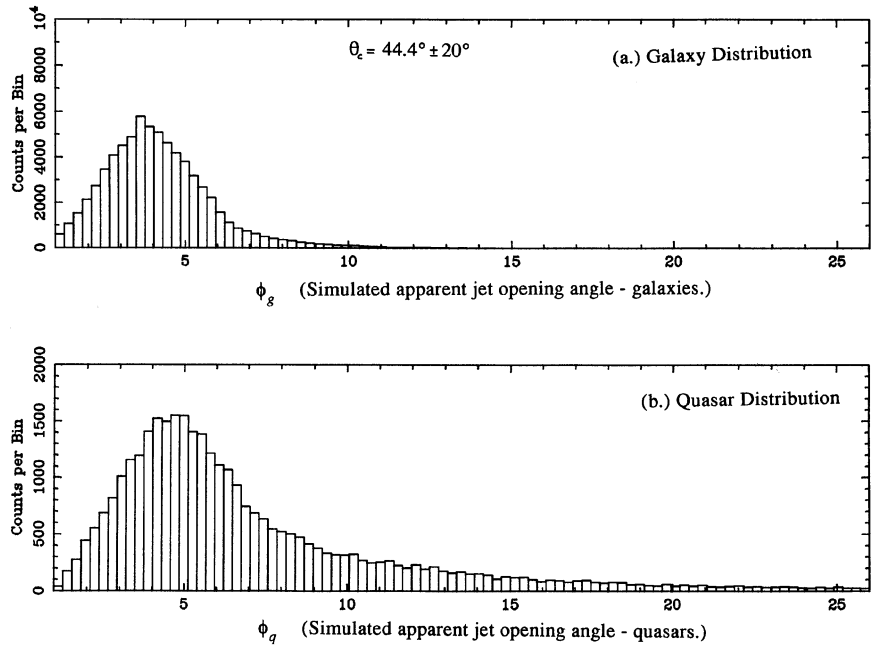

FIG. 10. Distributions of jet opening angles for Monte Carlo simulation with range of cutoff angles between $\theta=24.4°$ and 64.4° ($\theta_c=44.4°\pm20°$). Other details are the same as Fig. 4.

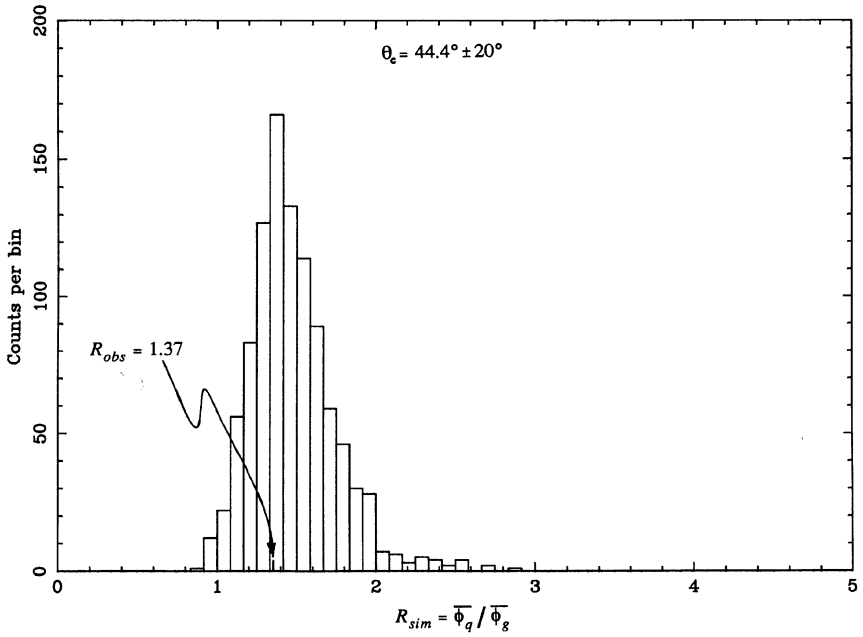

FIG. 11. Distribution of Monte Carlo simulated ratios $R_{\rm sim}$ assuming range of cutoff angles between $\theta=24.4°$ and 64.4° ($\theta_c=44.4°\pm20°$). Other details are the same as Fig. 5.

tions are used without redshift restriction [the first line of Table 2(b)] we find that the observed ratio ($R_{\rm obs}=1.37$) is about 1.6 standard deviations away from the mean simulated ratio, which places about 89% of the distribution closer to the most probable simulation ratio. When the upper limit measurements are excluded ($R_{\rm obs}=1.49$) we find that only about 71% of the range is closer to the most probable simulated ratio. These results show that the introduction of a 10° range in the cutoff angle improves the viability of the unified scheme. This improvement occurs because the median opening angle for the simulated galaxies increases, while having little effect in the median for the quasars, so that the $R_{\rm sim}$ distribution is shifted towards unity. Figures 8–11, and Tables 2(c) and 2(d) give results for even larger ranges in the cutoff angle. The largest range $44.4°\pm20°$ produces model distributions which are quite consistent with the observations. Hence, a unified scheme with a large scatter in the cutoff angle seems a better match to the observed opening angle distributions.

It has been suggested that in order to test the unified scheme, one must restrict one's sample by redshift, so that the quasars and galaxies have similar redshift distributions (Barthel 1989; Lonsdale 1993). This restriction serves to minimize the effects of cosmic evolution on the sources. For the sample used in the above discussion, the mean redshift of the galaxies is $\overline{z_g}\approx0.3$, while that of the quasars is $\overline{z_q}\approx1.1$, hence cosmic evolution could have a significant impact on the results. Barthel (1989) used only sources which fell within the range $0.5<z<1.0$ when testing his unified scheme. Longair (1985) reported that the redshift distribution of the quasars and galaxies are similar when $z>0.4$. The results of these redshift restrictions are also summarized in Table 2. When we restrict our sample this way, the number of observed galaxies and quasars drops, resulting in poorer statistics and broader distributions of the simulated ratios $R_{\rm sim}$. These broader $R_{\rm sim}$ distributions make it more difficult to discern any difference between the model and observations. For example, a redshift range $0.5<z<1.0$ gives $\overline{z_g}\approx\overline{z_q}\approx0.8$, but also reduces the sample sizes to six galaxies and four quasars. This observed sample has $R_{\rm obs}=1.61$, and the simplest model with a sharp cutoff angle gives $\overline{R_{\rm sim}}=2.34$. The difference between these values is not very significant, since the small sample size increases σ to 1.29, so that $R_{\rm obs}$ is within 0.57 standard deviations of $\overline{R_{\rm sim}}$ [Table 2(a)], and hence the observations and model are fairly consistent with being drawn from the same distribution. Extending the redshift range to $0.5<z<2.0$ brings in more objects, yet the model and observations remain reasonably consistent. Perhaps the only truly conclusive remark one can make, at least based on the existing data, is that the viability of the simplest unified scheme (sharp cutoff angle) is dependent upon the redshift restriction applied to the sample. Clearly, more data are needed before a precise test can be made using restricted redshift ranges.

We have not attempted to correct for the effects of cosmic evolution in galaxies and quasars. It may be possible to minimize the effects of this evolution by using narrow redshift ranges to limit the sample used in the test, but this certainly requires the presence of more data. Recently, however, Singal (1993) demonstrated that the extreme differences between the redshift and linear size distributions of quasars and galaxies could not be successfully explained by unification even when evolution is incorporated by allowing the cutoff angle in Barthel's (1989) model to vary with redshift. This might lead one to surmise that the dif-

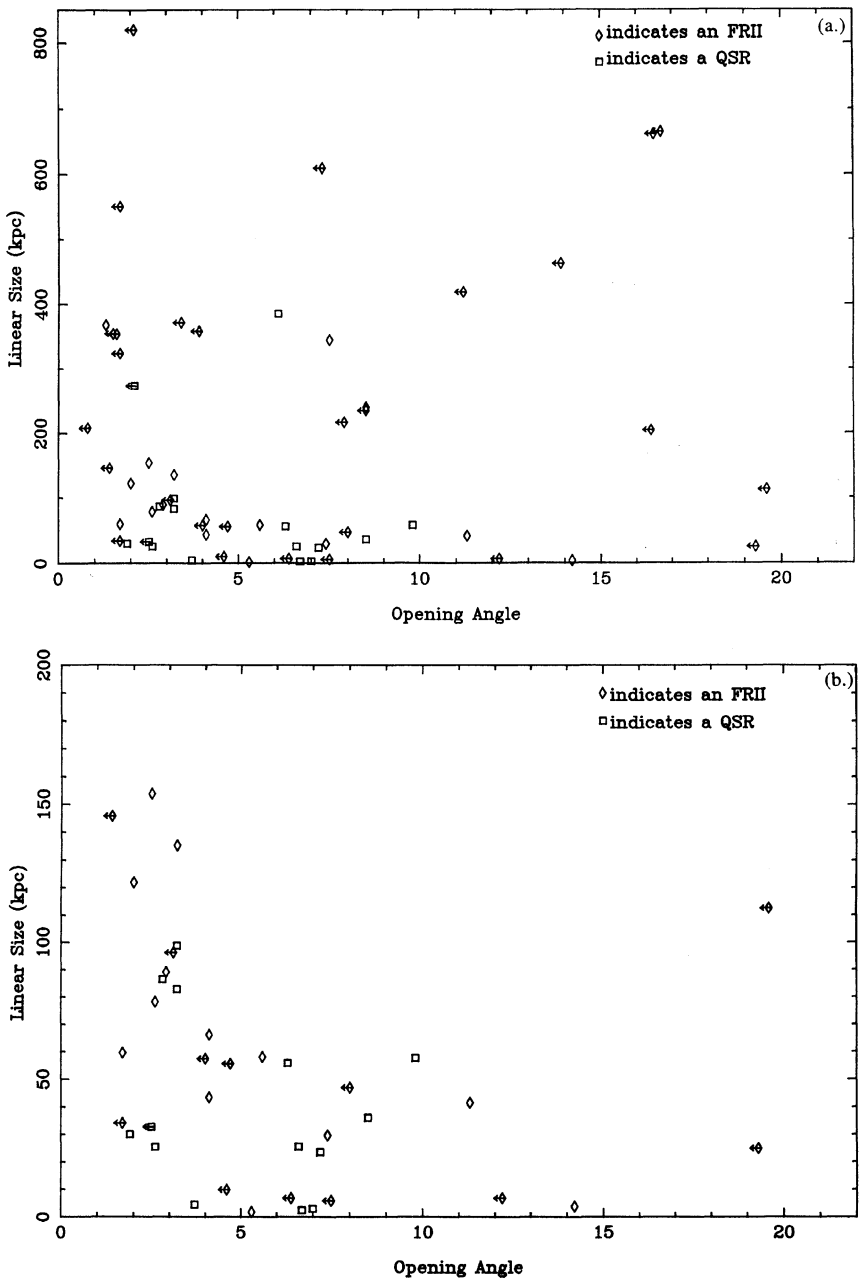

FIG. 12. Radio source linear size (kpc) vs jet opening angle (°) for observed sample of jets. Arrows are used to designate jet opening angles which are merely upper limits. (a) entire range of values; (b) enlargement of region near origin.

ferences in the success of the unified scheme, when put to the opening angle test presented here, are not, in fact, due to some excluded evolution, but rather the effect of looking at two separate populations of objects that may be unifiable in some other more elusive manner than simple orientation effects.

One possible source of error in this empirical test is that an orientation bias in our sample has been introduced by our studying only those sources for which high resolution maps are available. Because this selection effect has something to do with immensely complicated human behavior, it seems rather difficult to determine precisely how this might affect our results, but an attempt can be made. One possibility is that people studying jets might choose to image very bright ones, because they would be easier to study. Simple beaming models, however, suggest that brighter jets are the ones which are directed towards the viewer. This might mean that the jets we have studied here are biased towards having large opening angles. This is especially true in the case of the quasars, since these jets are supposed to be directed toward us, and thus would be over-represented in the sample. The only consequence this could have would

be to make our R_{obs} too high. Correcting this would increase the difference between R_{obs} and $\overline{R_{sim}}$, and hence tend to reduce the probability that the unification scheme is correct, especially the simplest version with a sharp cutoff.

An interesting comparison can be made between the use of opening angles as orientation indicators and the use of the linear size as an orientation indicator. Barthel (1989) used linear size for his empirical support of the unification scheme. We have measured the linear sizes of the objects we studied, in the same manner as Barthel. Like Barthel, we have doubled the size of all single-sided sources. In calculating the linear sizes, we assumed $H_0=75$ km s^{-1} Mpc^{-1} and $q_0=0.5$ in a standard Einstein–de Sitter model of the universe. Figure 12 contains a plot of linear size versus opening angle. The arrows on the graph indicate the opening angle measurements which are merely upper limits. We find a very loose anticorrelation between the parameters to the extent that there are no objects with large linear size and large opening angle. It is a little stronger for the sources under 200 kpc in size [Fig. 12(b)]. This anticorrelation is expected if the two parameters are indeed orientation indicators: One would not expect a source with high linear size to have a large opening angle. Removal of the large upper limit values, which contain little information, gives further support for this anticorrelation. The discovery of this anticorrelation should be a comfort to those using source linear size to support unification. The looseness of the anticorrelation, extremely evident in the graph, can be explained by an intrinsic spread in either, or both, parameters or perhaps by merely stating that the two parameters are affected differently by the surrounding environment of galaxies and quasars.

7. CONCLUSIONS

We have outlined a test of unified models in which jet opening angles are used as orientation indicators, and then applied this test to the available data. The unified model predicts that the opening angles of quasar jets should tend to be larger than those of the FRII galaxies, and this is indeed what is observed for the available data. A detailed comparison of the unified model and the observations shows that the predicted ratio of quasar to galaxy opening angle is actually too large, unless there is a large scatter in the "cutoff" angle which divides quasars from galaxies. If we attempt to minimize the effects of cosmic evolution, and restrict the observed sample to $0.5<z<1.0$ (Barthel 1989), the sample size is reduced and it becomes statistically difficult to discern any difference between the unified scheme and the available data. More data are required to improve the statistical significance of our test; it would also be desirable to include cosmic evolution effects within the unified scheme. Finally, we demonstrate the existence of an anticorrelation between observed jet opening angle and source linear size, which supports the validity of these parameters as orientation indicators.

We are indebted to Alan Bridle, Jacqueline Van Gorkum and Chris Salter for helpful discussions, to Ashok Singal for his correct derivation of the apparent (observed) opening angle, and to an anonymous referee for useful comments which improved the presentation of results. B.R.O. acknowledges the support of the NRAO Summer Research Assistantship Program.

REFERENCES

Antonucci, R. R. J. 1985, ApJS 59, 499
Barthel, P. D. 1989, ApJ, 336, 606
Barthel, P. D., Schilizzi, R. T., Miley, G. K., Jaegers, W. J., & Strom, R. G. 1985, A&A, 148, 243
Black, A. R. S., Baum, S. A., Leahy, J. P., Perley, R. A., Riley, J. M., & Scheuer, P. A. G. 1992, MNRAS, 256, 186
Bridle, A. H., Fomalont, E. B., Palimaka, J. J., & Willis, A. G. 1981a, ApJ, 248, 499
Bridle, A. H., Fomalont, E. B., & Cornwell, T. J. 1981b, AJ, 86, 1294
Bridle, A. H., Perley, R. A., & Henriksen, R. N. 1986, AJ, 92, 535
Browne, I. W. A., Orr, M. J. L., Davis, R. J., Foley, A., Muxlow, T. W. B., & Thomasson, P. 1982, MNRAS, 198, 673
Burns, J. O., Schwendeman, E., & White, R. A. 1983, ApJ, 271, 575
Davis, R. J., Muxlow, T. W. B., & Conway, R. G. 1985, Nature, 318, 343
Eilek, J. A., Burns, J. O., O'Dea, C. P., & Owen, F. N. 1984, ApJ, 278, 37
Fanti, C., Fanti, R., de Ruiter, H. R., & Parma, P. 1987, A&AS, 69, 57
Fanti, C., *et al.* 1989, A&A, 217, 45
Fernini, I. 1992, Ph.D thesis, New Mexico State University
Fernini, I., Leahy, J. P., Burns, J. O., & Basart, J. P. 1991, ApJ, 381, 63
Heckman, T. M., Miley, G. K., Balick, B., van Breugel, W. J. M., & Butcher, H. R. 1982, ApJ, 262, 529
Jaegers, W. J. 1987, A&AS, 67, 395
Kollgaard, R. I., Wardle, J. F. C., & Roberts, D. H. 1989, AJ, 97, 1551
Kollgaard, R. I., Wardle, J. F. C., & Roberts, D. H. 1990, AJ, 100, 1057
Leahy, J. P. 1984, MNRAS, 208, 323
Leahy, J. P., Jaegers, W. J., & Pooley, G. G. 1986, A&A, 156, 234
Linfield, R., & Perley, R. 1984, ApJ, 279, 60
Longair, M. S. 1985, in Radio Astronomy and the Physics of the Universe, edited by R. Fanti, G. Grueff, and G. Setti (Instituto di Radioastronomia del CNR, Bologna), p. 25
Lonsdale, C. 1993, private communication
Mantovani, F., Saikia, D. J., Browne, I. W. A., Fanti, R., Muxlow, T. W. B., & Padrielli, L. 1990, MNRAS, 245, 427
O'Dea, C. P., Barvainis, R., & Challis, P. M. 1988, AJ, 96, 435
Owen, F. N., O'Dea, C. P., Inoue, M., & Eilek, J. A. 1985, ApJ, 294, L85
Padovani, P., & Urry, C. M. 1992, ApJ, 387, 449
Pearson, T. J., Perley, R. A., & Readhead, A. C. S. 1985, AJ, 90, 738
Perley, R. A., Dreher, J. W., & Cowan, J. J. 1984, ApJ, 285, L35
Pooley, G. G., Leahy, J. P., Shakeshaft, J. R., & Riley, J. M. 1987, MNRAS, 224, 847
Saikia, D. J., Junor, W., Cornwell, T. J., Muxlow, T. W. B., & Shastri, P. 1990, MNRAS, 245, 408
Saikia, D. J., Salter, C. J., & Muxlow, T. W. B. 1987, MNRAS, 224, 911
Singal, A. K. 1993, MNRAS, 262, L37
Spencer, R. E., *et al.* 1991, MNRAS, 250, 225
Strom, R. G., Riley, J. M., Spinrad, H., van Breugel, W. J. M., Djorgovski, S., Liebert, J., & McCarthy, P. J. 1990, A&A, 227, 19
Swarup, G., Sinha, R. P., & Hilldrup, K. 1984, MNRAS, 280, 813
Swarup, G., Sinha, R. P., & Saikia, D. J. 1982, MNRAS, 201, 393
van Breugel, W., & Fomalont, E. B. 1984, ApJ, 282, L55
Wrobel, J. M., & Lind, K. R. 1990, ApJ, 348, 135